Limnol. Oceanogr., 55(6), 2010, 2246–2261

doi:10.4319/lo.2010.55.6.2246

The isotopic and hydrologic response of small, closed-basin lakes to climate forcing from predictive models: Simulations of stochastic and mean-state precipitation variations

Byron A. Steinman,* Michael F. Rosenmeier, and Mark B. Abbott

Department of Geology and Planetary Science, University of Pittsburgh, Pittsburgh, Pennsylvania

Abstract

A hydrologic and isotope mass-balance model is applied to two small, closed-basin lakes, Castor and Scanlon, in north-central Washington to describe the influence of hydroclimatic forcing on lake hydrologic and isotopic evolution. Simulations of lake responses to the combined effects of stochastic variability (i.e., random interannual fluctuations) and long-term (i.e., multidecade to century), mean-state changes in precipitation were conducted using 300 yr of randomly generated precipitation data as model inputs. Simulation results demonstrate that average (long-term) closed-basin, lake-water, oxygen-isotope values are dependent largely upon lake-water outseepage (i.e., subsurface outflow) rates, with lower (higher) outseepage resulting in decreased (increased) isotopic sensitivity to long term precipitation changes, and that the lake basin surface-area-to-volume (SA : V) ratio changes with depth influence the direction of the isotopic response. Simulation results also suggest that, as average lake volume decreases as a consequence of decreasing mean-state precipitation amounts, interannual lake-water isotopic variability in response to stochastic forcing will increase. Conversely, as the average lake volume increases in response to increasing mean-state precipitation amounts, interannual lake-water isotopic variations associated with stochastic forcing will decrease. Additional model experiments demonstrate that increased (decreased) variance in precipitation leads to increased (decreased) water volume within lakes over the long term, which (if stochastic variance changes are large enough) could result in decreased (increased) lake-water oxygen-isotopic sensitivity to stochastic precipitation.

The oxygen isotope composition of closed-basin lake water is controlled by many factors including net groundwater flux, catchment size and soil characteristics, lake basin morphology, and hydroclimatic forcing through stochastic variability (i.e., random interannual fluctuations), and mean-state changes (i.e., changes in multidecade to century averages) in precipitation, relative humidity, and temperature (Gat 1970; Leng 2004; Steinman et al. 2010). In regions with highly seasonal climates such as the Pacific Northwest, precipitation and evaporation rates substantially vary intra-annually, whereas lake-basin morphology, lake seepage rates, and catchment hydrologic parameters such as soil thickness and depth, vary only on decadal and longer time scales, largely in response to interannual climate forcing (Johnson and Watson-Stegner 1987; Phillips 1993; Rosenmeier et al. in press). Changes in average climatic states, such as long-term increases in the variance of precipitation about an established annual mean, or the shifting of precipitation from one season to another, add additional complexity to the geochemical evolution and, more specifically, the isotopic composition, of lake water (Vassiljev 1998; Leng et al. 2001; Pham et al. 2009). Only by simulating lake sensitivity to these factors using quantitative models can the isotopic response of closed-basin lakes to climate change be predicted, a fact that has considerable relevance to paleoclimate interpretations of sediment core oxygen isotope ($\delta^{18}O$) records (Ricketts and Johnson 1996; Cross et al. 2001; Jones et al. 2005).

* Corresponding author: bas68@pitt.edu

Groundwater flow regimes and associated lake seepage rates are of particular importance in the control of steady-state lake-water $\delta^{18}O$ values (Donovan et al. 2002; Smith et al. 2002; Shapley et al. 2008). In closed-basin systems that are isolated from regional groundwater (i.e., perched lakes), the origin of subsurface inflow is often precipitation falling on or very near the catchment (Almendinger 1993). In seasonal climates, under these conditions, base flow has an isotopic composition that is approximately equal to the weighted average isotopic composition of mean annual precipitation and, therefore, can effectively be considered runoff with an extended transit time (Henderson and Shuman 2009). In contrast, subsurface inflows to lake systems that are not isolated from regional groundwater aquifers can potentially undergo a much more complex isotopic evolution during transport to a lake (Smith et al. 1997).

Subsurface outflow from closed-basin lakes occurs as seepage through the lake bed at rates that are typically very low due to the low hydraulic conductivity of silt and clay-rich lake sediment. Outseepage, a potentially minimal hydrologic flux, is in all cases a fundamental control on the steady-state isotopic composition of closed-basin lake water because, through interaction with lake-basin morphology, it determines the proportion of water that leaves a lake through fractionating (evaporation) and nonfractionating (outseepage) pathways (Steinman et al. 2010).

In this study, a numeric, hydrologic and isotope mass-balance model was applied to Castor and Scanlon Lakes, north-central Washington, and was used to simulate lake-water hydrologic and isotopic responses to changes in

mean-state and stochastic precipitation. In the first set of experiments, intra-annual variations in lake depth and $\delta^{18}O$ values, as well as interannual lake transient and steady-state responses to mean-state precipitation forcing, were simulated by applying long-term increases and decreases ($\pm$ 50%) in monthly precipitation values. In the second set of experiments, the model structure was modified to include stochastic changes in precipitation, in order to more realistically simulate hydroclimatic forcing conditions. In this series of tests, a precipitation data set was randomly generated using the mean and standard deviation of 20th-century precipitation values recorded at local weather stations and applied over three 100-yr periods during which varying long-term precipitation changes were used to simulate the gradual shift from one hydroclimatic mean state to another. To augment these analyses, and to test model-derived hypotheses across a diversity of lake morphologies and hydrologic settings, model simulations were also conducted on two hypothetical, hypsographically and hydrologically distinct lakes, representing variations on both Castor and Scanlon Lakes. In the third series of experiments, the standard deviation of interannual precipitation forcing factors (established in the second series of tests) was varied over three 100-yr periods in order to simulate the lakes' hydrologic and isotopic responses to changes in the variance of stochastic variability in the absence of mean-state forcing.

Methods

Study sites and regional climate—Scanlon Lake (SL) and Castor Lake (CL) are located in the Limebelt region of north-central Washington on a terrace margin of the Okanogan River. The lake catchments are small (< 1 km^2) and occupy a topographic high isolated from regional groundwater. Climate in the area is seasonal, semiarid, and largely controlled by the interaction between the Pacific westerly winds and the Aleutian low-pressure system and north Pacific high-pressure system.

Model structure—The hydrologic and isotope mass-balance of CL and SL are calculated in the model using the following equations:

$$\frac{dV_L}{dt} = \Sigma I - \Sigma O \tag{1}$$

$$\frac{d(V_L \delta_L)}{dt} = \Sigma I \delta_I - \Sigma O \delta_O \tag{2}$$

where V_L is lake volume, ΣI and ΣO are the total surface and below ground inflows to and outflows from the lakes, and δ is the isotopic composition of the inflows and outflows. These equations provide the basis for a system of 12 ordinary differential equations, compiled using Stella (isee systems) software, that describe water and isotope dynamics for the lake catchment systems. More specifically, the hydrologic model is defined by six separate differential equations corresponding to unique water reservoirs (catchment groundwater, snowpack, shallow and deep lake volumes, etc.). Volumetric fluxes to the reservoirs are described by model subroutines for lake stratification, soil-moisture availability, snowpack, and surface and subsurface inflows. Additional detail regarding calculation of the flux components as well as all other aspects of the model is provided by Steinman et al. (2010). All model simulations were conducted with the Stella software using the fourth-order Runge-Kutta numerical integration method.

Mean-state precipitation forcing simulation structure—In the first series of model simulations, monthly average climate data and modern catchment parameter data sets were used to approximate the monthly and seasonal variability of CL and SL water levels, and to evaluate the transient (i.e., short-lived) and longer term, steady-state sensitivity of the lakes to precipitation changes. Each set of sensitivity simulations was conducted on a monthly time step over $\sim$ 63 model years, using modern catchment parameters and average climate data for the 20th century. At simulation month 501, the precipitation rate was either increased or decreased by 50% and maintained at the altered value for the remainder of the test in order to simulate large changes in mean hydroclimatic conditions.

Stochastic precipitation forcing simulation structure—To explore the interplay between stochastic variability and mean-state change in hydroclimate on closed-basin lake-water balance and $\delta^{18}O$ values, hydrologic forcing simulations were conducted in which randomly adjusted precipitation rates (i.e., stochastic variations in precipitation) were superimposed upon long-term changes in mean precipitation levels. Specifically, for each simulation year, a forcing factor was produced using a random number algorithm and applied to each month during the year. Random forcing factors were generated using a standard deviation equal to the coefficient of variation of annual precipitation over the 20th century (0.28) calculated from local weather station data sets (Steinman et al. 2010). This method is fundamentally similar to that of the more sophisticated daily stochastic weather generators applied by global climate models but is simpler because randomness in monthly, rather than daily, precipitation and only one climate variable (in this case, precipitation) are simulated (Richardson 1981; Katz 1996; Mearns et al. 1997).

For the combined mean-state and stochastic variability tests, steady-state conditions were achieved during the first 25 yr of each experiment, after which precipitation rates were randomly adjusted on an interannual basis, as described above, to simulate stochastic climate variability. During the first 100-yr simulation period (i.e., during model years 25 to 125), no mean-state precipitation forcing was applied. In the subsequent 100-yr period (model years 125–225), the average precipitation value was gradually increased or decreased toward a fixed percentage ($\pm$ 50% of modern) to simulate variation in the mean hydroclimate state. During the third 100-yr simulation period (model years 225–325), precipitation values were held at the adjusted mean-state value (again, either 50% above or

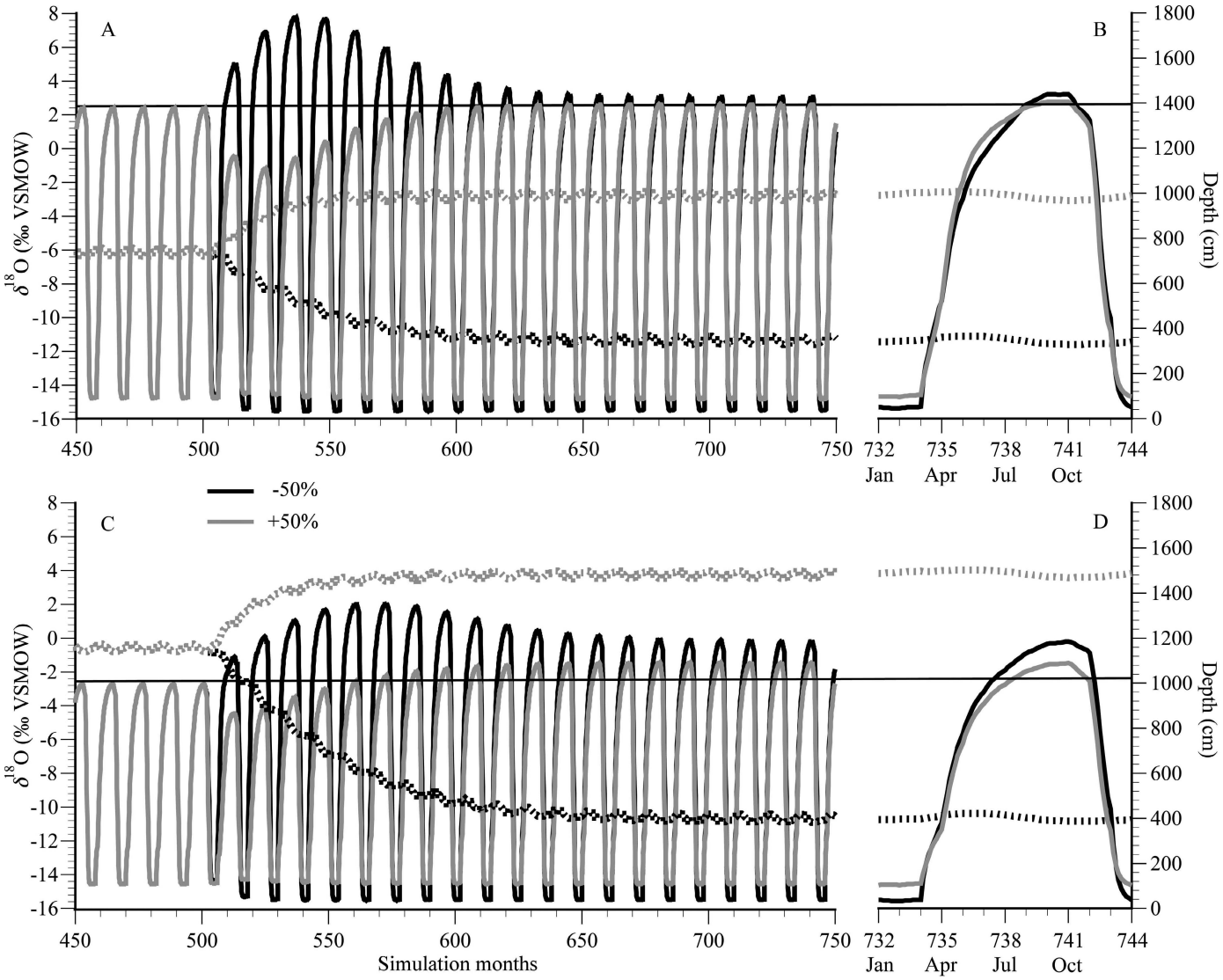

Fig. 1. Depth (dashed lines) and lake-water $\delta^{18}O$ value changes (solid lines) at SL and CL in response to mean-state precipitation increases of 50% (gray lines) and decreases of 50% (black lines) over model simulation months 450 to 750 (A and C, respectively) with an expanded view of model months 732–744 (B and D, respectively) following reestablishment of steady state. In both lake simulations precipitation changes were initiated at month 501.

below modern) achieved at model year 225 to simulate the effects of stochastic variability within an altered long-term average precipitation amount. Only 1 set of 100 stochastic forcing factors was applied in each simulation in order to ensure that the standard deviation of precipitation values in each simulation period were identical and to thereby maintain consistency in the simulations.

Similarly, to investigate the influence of changes in the variance of stochastic forcing in the absence of mean-state change, simulations were conducted in which the standard deviation of randomly adjusted precipitation rates was increased over the course of the tests. The general structure of the stochastic forcing variance change simulations was identical to the combined mean-state and stochastic forcing simulations, with the exceptions that no mean-state forcing was applied and that the standard deviation of the precipitation forcing factors increased from 0.21 to 0.35 (i.e., from −25% to +25% of 0.28, the 20th-century coefficient of variation of precipitation) from the first to the third simulation periods, respectively.

Results

Simulation of mean-state precipitation forcing—Steady-state simulations predicted extensive intra-annual isotopic variability at SL (Fig. 1A,B) and CL (Fig. 1C,D), with $\delta^{18}O$ variations of approximately 17‰ and 12‰, respectively, between winter and summer months and a maximum summer $\delta^{18}O$ value at SL ~ 5‰ greater than that of CL prior to precipitation forcing at model month 501. These predictions are consistent with modern observations of intra-annual hydrologic and isotopic variability at CL and SL (Steinman et al. 2010).

After a 50% decrease in precipitation at month 501, both CL and SL exhibited transient annual maximum $\delta^{18}O$ increases of $\sim$ 5‰ and 6‰, respectively, with CL taking longer (relative to SL) to achieve transient maxima and steady-state $\delta^{18}O$ values. In contrast, after a 50% increase in precipitation, both CL and SL exhibited short-lived maximum annual $\delta^{18}O$ decreases of $\sim$ 2‰ and 4‰, respectively. After achieving transient maxima or minima, annual $\delta^{18}O$ values at both lakes transitioned to new steady-state values corresponding to the precipitation change initiated at month 501. In the decreased precipitation scenario, new annual maximum steady-state $\delta^{18}O$ values were higher than the values prior to precipitation forcing, although the values at CL were appreciably higher than at SL (an increase of $\sim$ 2.6‰ and 0.7‰, respectively). In the increased precipitation scenario, new steady-state $\delta^{18}O$ values were also higher than the values prior to precipitation forcing, although the increase at SL ($\sim$ 0.2‰) was significantly smaller than that of CL ($\sim$ 1.3‰).

Simulation of combined mean-state and stochastic precipitation forcing—During the course of the SL simulations, stochastic variability in precipitation led to large interannual fluctuations in average summer (June–August) lake volume and $\delta^{18}O$ values. In the mean-state precipitation decrease scenario, the magnitude of these fluctuations increased during the second 100-yr simulation period and reached a maximum during the third simulation period (Fig. 2; Table 1). Conversely, in the precipitation increase scenario, the magnitude of these fluctuations decreased during the second 100-yr simulation period and reached a minimum during the third simulation period (Fig. 3). In response to mean-state precipitation change, SL summer average $\delta^{18}O$ values increased slightly over the course of both simulations, with a larger magnitude increase occurring during the precipitation reduction scenario (Table 1).

The response of CL to stochastic variability in precipitation was similar to that of SL, in that the magnitude of interannual $\delta^{18}O$ and lake-volume changes increased from the first to the third simulation period in response to a mean-state precipitation decrease (Fig. 4; Table 1). In the precipitation increase scenario, the smallest magnitude interannual $\delta^{18}O$ and volume changes occurred during the third 100-yr period (Fig. 5; Table 1). The response of CL to mean-state precipitation changes was, however, different than that of SL, in that average summer $\delta^{18}O$ values substantially increased from one simulation period to the next in response to mean-state precipitation increases and decreases.

At both CL and SL, large changes in residence time, surface-area-to-volume (SA : V) ratio values, and outflow proportions occurred in response to both stochastic and mean-state precipitation variability forcing (Figs. 2–5; Table 1). In all cases, residence time values exhibited a strong association with lake SA : V ratio values and evaporative outflow proportions, with residence times decreasing in response to increases in evaporative outflow proportions and SA : V ratio values.

Simulation of combined mean-state and stochastic precipitation forcing within hypothetical lakes—Model simulations were also conducted on two hypothetical lakes, representing variations on the bathymetric and outseepage characteristics of Castor and Scanlon Lakes, and denoted CL2 and SL2, respectively. In the CL2 configuration, SA : V ratio values above a depth of 12 meters were changed such that values decreased with increasing depth (from the actual, opposite, configuration of increasing values with depth increases). In the SL2 configuration the seepage rate was increased to 1.5 times that of CL to a value of 2.4% of monthly lake volume (Steinman et al. 2010).

In the CL2 configuration, the $\delta^{18}O$ response to stochastic variability forcing was similar to that of CL, with standard deviations for both configurations within 0.1‰ for all three simulation periods (Fig. 6; Table 1). The lake-water $\delta^{18}O$ response to a mean-state precipitation increase was dissimilar, however, with a lower average value (relative to the actual bathymetric configuration of Castor Lake) during the third simulation period. In the CL2 configuration, the SA : V ratio over the third simulation period decreased in response to increasing volume while seepage and evaporation outflow proportions increased and decreased, respectively.

The lake-water $\delta^{18}O$ response to stochastic variability in the SL2 model test was also similar to that of SL, with standard deviations for both configurations within 0.4‰ over all three simulation periods (Fig. 7; Table 1). The $\delta^{18}O$ responses of lake water to mean-state precipitation forcing likewise differed, with the average $\delta^{18}O$ value in the SL2 configuration appreciably lower in all three simulation periods and increasing from one period to the next. Seepage and evaporation outflow proportions of total lake volume were also markedly different between the true Scanlon Lake and SL2 configurations, with a higher outseepage proportion and a lower evaporation proportion in the SL2 configuration over all three simulation periods.

Simulation of variance changes in stochastic precipitation forcing—In the case of both CL and SL, changes in the standard deviation of interannual precipitation forcing led to commensurate changes in the standard deviation of interannual lake-water $\delta^{18}O$ values and volume changes (Figs. 8, 9; Table 1). No large-scale deviations from mean-state values for any of the analyzed lake parameters were observed with the exception of lake volume, which increased by approximately 6% at SL and 3% at CL between the first and third simulation periods.

Discussion

Lake responses to mean-state precipitation forcing—Mean-state precipitation simulation results demonstrate that SL has a higher maximum annual $\delta^{18}O$ value relative to CL as a result of the larger proportion of water lost through evaporation, a fractionating pathway, in comparison to outseepage, a nonfractionating pathway (Table 1) (Steinman et al. 2010). SL also exhibits a stronger transient response to precipitation forcing. The slower equilibration time of CL occurs because the higher residence time,

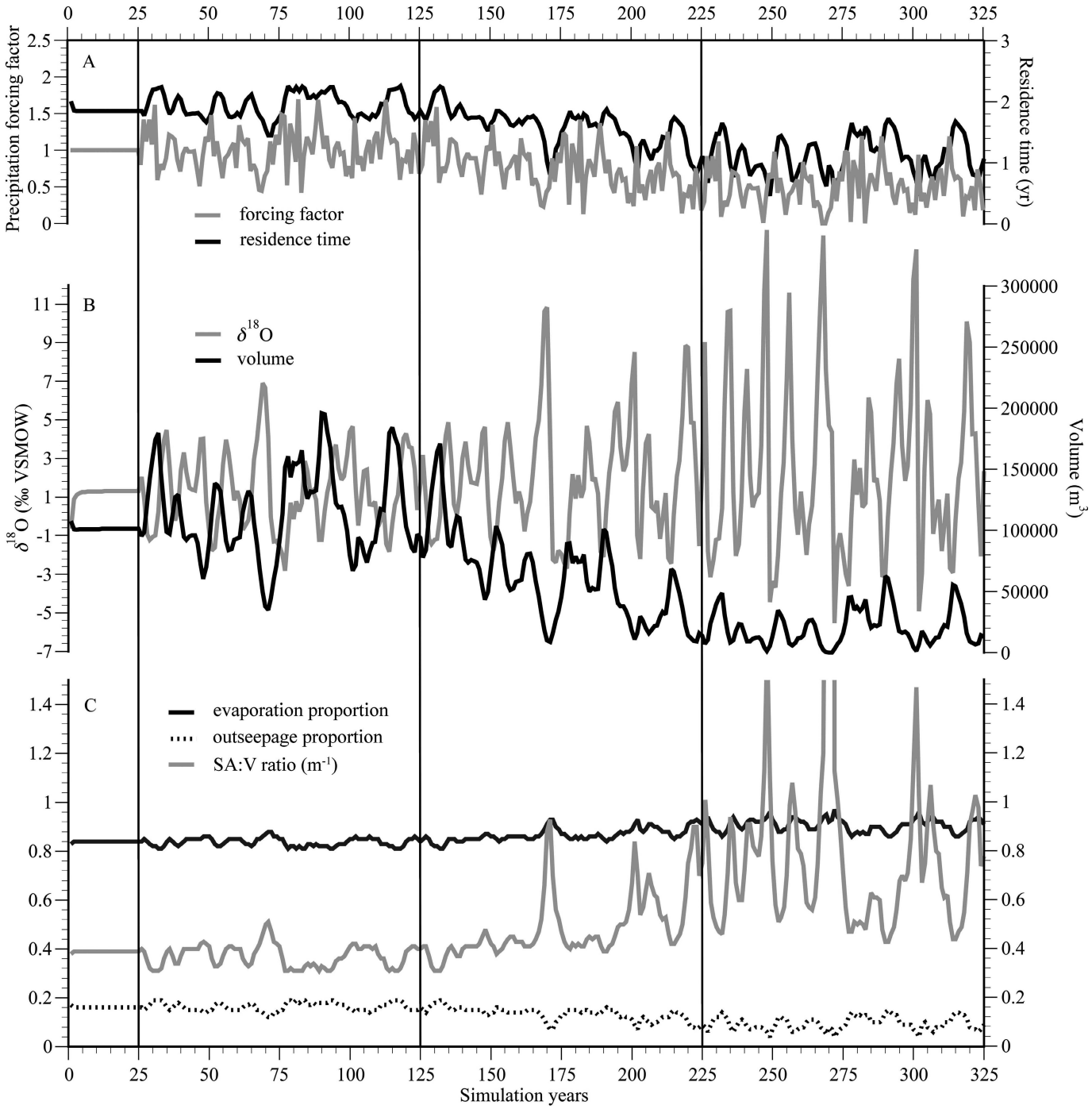

Fig. 2. SL responses to the superimposition of stochastic variations and a mean-state precipitation decrease of 50%. Between years 0 and 25, no changes in precipitation were applied. Between years 25 and 125, precipitation was varied stochastically with a mean and standard deviation equal to observed 20th-century values. Between years 125 and 225, mean-state precipitation was incrementally decreased by 50% while maintaining stochastic variations applied in years 25–125. Between years 225 and 325, mean-state precipitation was maintained at a value 50% below the 20th-century average while again maintaining the stochastic variations applied in the prior 100-yr simulation periods. (A) Superimposed stochastic and mean-state precipitation forcing factors (gray line) and residence times (black line). (B) Average summer (June–August) surface-water δ^{18}O values (gray line) and lake volumes (black line) resulting from described precipitation changes. (C) Lake SA : V ratio values (gray line) and the proportions of water lost to evaporation (black line) and outseepage (dashed line). Vertical lines delineate 100-yr simulation periods identified in Table 1.

Table 1. Average summer (June–August) values for lake variables for each simulation (sim.) period in response to stochastic and mean-state precipitation variations.

Mean precipitation change	Sim. period	Volume (m^3)	Average inter-annual % volumetric change	Depth (cm)	Surface lake $\delta^{18}O$ (‰)	Surface lake $\delta^{18}O$ standard deviation (‰)	Evaporation proportion	Outseepage proportion	SA : V ratio (m^{-1})	Residence time (yr)
CL										
0.5 (−50%)	1	311,529	9.1	1165	−3.38	1.36	0.53	0.47	0.19	2.43
	2	183,828	14.8	857	−2.65	2.36	0.58	0.42	0.24	2.17
	3	62,778	35.2	460	−1.13	4.05	0.72	0.28	0.50	1.48
1.5 (+50%)	1	311,529	9.1	1165	−3.38	1.36	0.53	0.47	0.19	2.43
	2	437,107	7.3	1337	−3.09	1.10	0.55	0.45	0.20	2.32
	3	573,361	5.1	1480	−2.46	0.69	0.58	0.42	0.23	2.18
SL										
0.5 (−50%)	1	114,216	11.7	762	1.33	1.99	0.84	0.16	0.37	1.94
	2	60,339	19.4	581	1.94	2.91	0.87	0.13	0.49	1.58
	3	20,600	43.6	372	2.37	4.64	0.91	0.09	0.76	1.12
1.5 (+50%)	1	114,216	11.7	762	1.33	1.99	0.84	0.16	0.37	1.94
	2	174,936	8.5	887	1.19	1.48	0.83	0.17	0.34	2.05
	3	230,052	5.1	980	1.65	0.74	0.84	0.16	0.36	1.96
CL2										
1.5 (+ 50%)	1	326,003	9.3	1196	−3.74	1.41	0.51	0.49	0.17	2.53
	2	508,880	7.2	1463	−4.32	1.10	0.48	0.52	0.15	2.70
	3	739,698	4.6	1747	−4.65	0.70	0.45	0.55	0.13	2.88
SL2										
0.5 (−50%)	1	71,467	15.6	641	−1.31	1.73	0.64	0.36	0.43	1.26
	2	39,764	26.0	494	−0.42	2.73	0.69	0.31	0.57	1.08
	3	14,752	53.5	323	0.83	4.25	0.77	0.23	0.90	0.81
CL*										
−25%	1	307,005	7.0	1164	−3.51	1.03	0.53	0.47	0.18	2.45
0	2	310,366	9.3	1163	−3.40	1.37	0.53	0.47	0.19	2.43
+25%	3	315,256	11.6	1164	−3.26	1.72	0.54	0.46	0.19	2.41
−25%	1	110,168	9.13	756	1.27	1.54	0.84	0.16	0.37	1.93
0	2	113,633	12.0	761	1.32	2.00	0.84	0.16	0.37	1.94
+25%	3	116,792	14.7	765	1.42	2.47	0.84	0.16	0.37	1.94

* Stochastic forcing variance change simulations. Percentage change in the standard deviations for each 100-yr period are displayed in the mean precipitation change column.

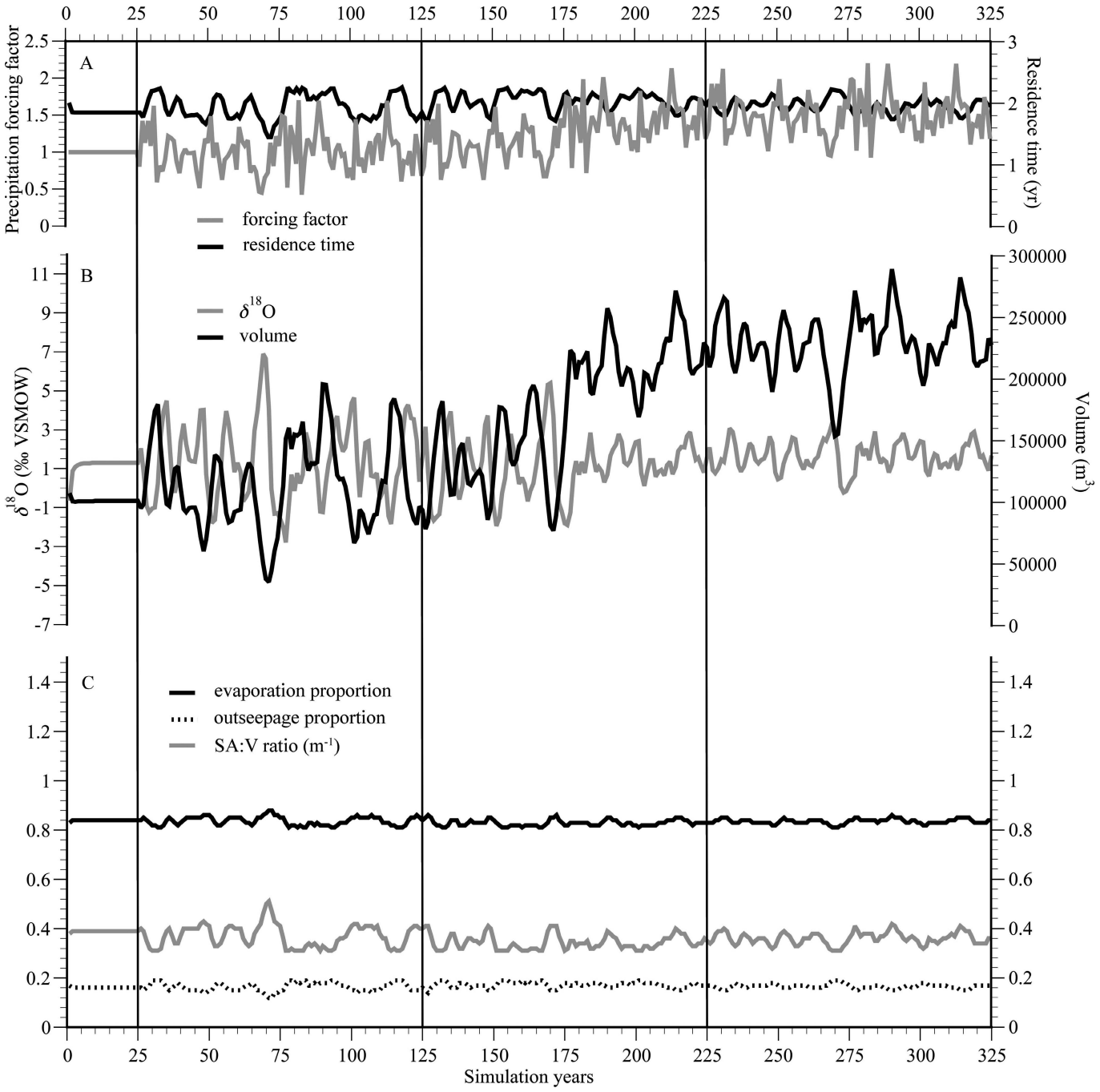

Fig. 3. SL responses to the superimposition of stochastic variations and a mean-state precipitation increase of 50%. Between years 0 and 25, no changes in precipitation were applied. Between years 25 and 125, precipitation was varied stochastically, with a mean and standard deviation equal to observed 20th-century values. Between years 125 and 225, mean-state precipitation was incrementally increased by 50% while maintaining stochastic variations applied in years 25–125. Between years 225 and 325, mean-state precipitation was maintained at a value 50% above the 20th-century average while again maintaining stochastic variations applied in the prior 100-yr simulation periods. (A) Superimposed stochastic and mean-state precipitation forcing factors (gray line) and residence times (black line). (B) Average summer (June–August) surface-water δ^{18}O values (gray line) and lake volumes (black line) resulting from described precipitation changes. (C) Lake SA : V ratio values (gray line) and the proportions of water lost to evaporation (black line) and outseepage (dashed line).

greater volume, and the relatively low SA : V ratio result in interannual volumetric fluxes that are, in proportion to lake volume, smaller. This in turn results in a less pronounced transient lake-water δ^{18}O response and a slower return to steady-state conditions. Additionally, CL exhibits a posttransient maximum annual steady-state δ^{18}O value that is, in both positive and negative forcing scenarios, larger relative to the preforcing value, while

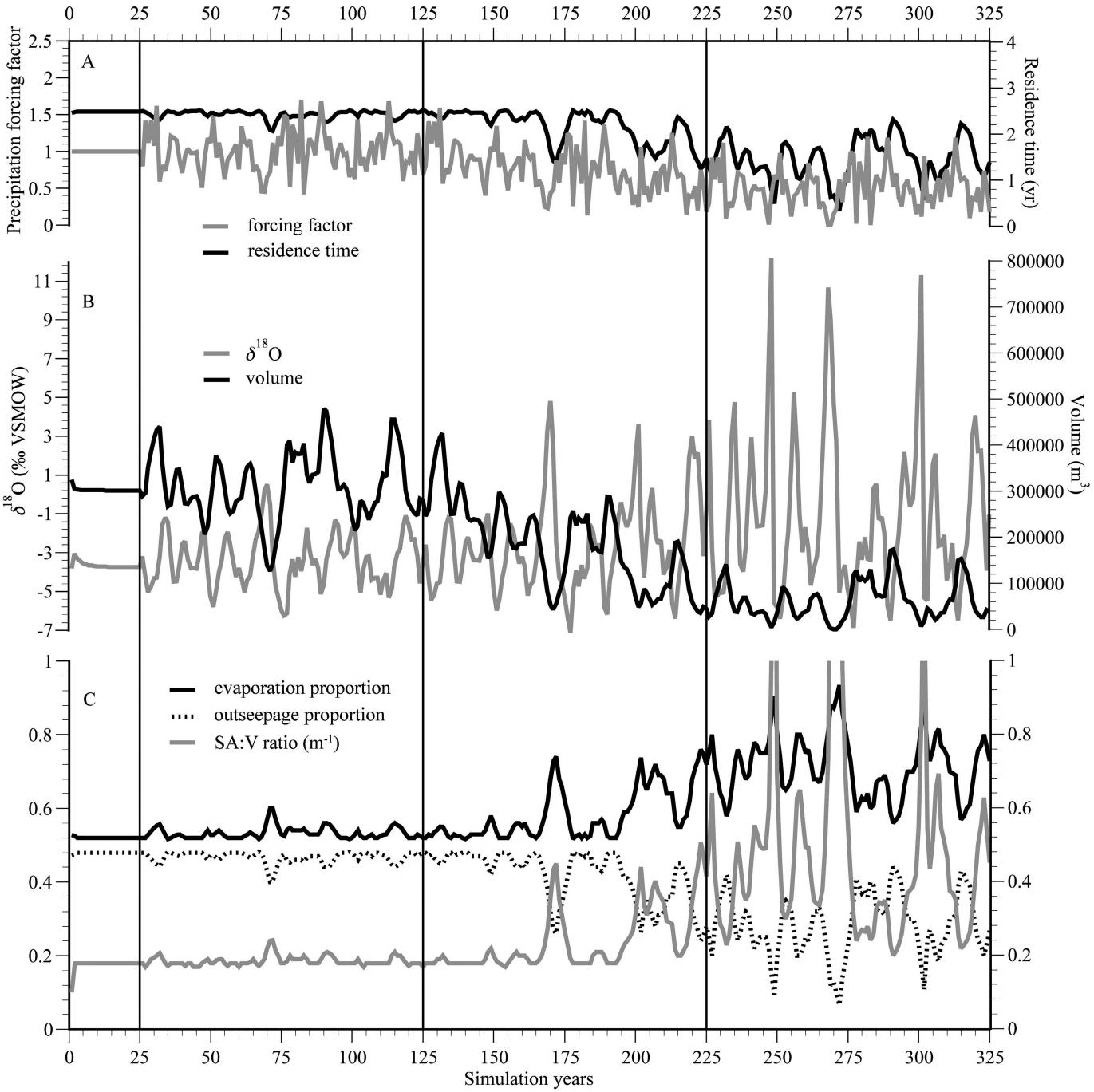

Fig. 4. CL responses to the superimposition of stochastic variations and a mean-state precipitation decrease of 50%. Between years 0 and 25, no changes in precipitation were applied. Between years 25 and 125, precipitation was varied stochastically with a mean and standard deviation equal to observed 20th-century values. Between years 125 and 225, mean-state precipitation was incrementally decreased by 50% while maintaining stochastic variations applied in years 25–125. Between years 225 and 325, mean-state precipitation was maintained at a value 50% below the 20th-century average while again maintaining stochastic variations applied in the prior 100-yr simulation periods. (A) Superimposed stochastic and mean-state precipitation forcing factors (gray line) and residence times (black line). (B) Average summer (June–August) surface-water δ^{18}O values (gray line) and lake volumes (black line) resulting from described precipitation changes. (C) Lake SA : V ratio values (gray line) and the proportions of water lost to evaporation (black line) and outseepage (dashed line).

SL, in contrast, exhibits a posttransient maximum annual steady-state value that is nearly identical to the preforcing value (Fig. 1). This is again due to disparities in the outflow proportions, in that the greater proportion of seepage outflow at CL (and the consequently smaller evaporative outflow proportion) result in a greater sensitivity of steady-state δ^{18}O values to SA : V ratio changes with changing depth. Specifically, as lake level either increases or decreases

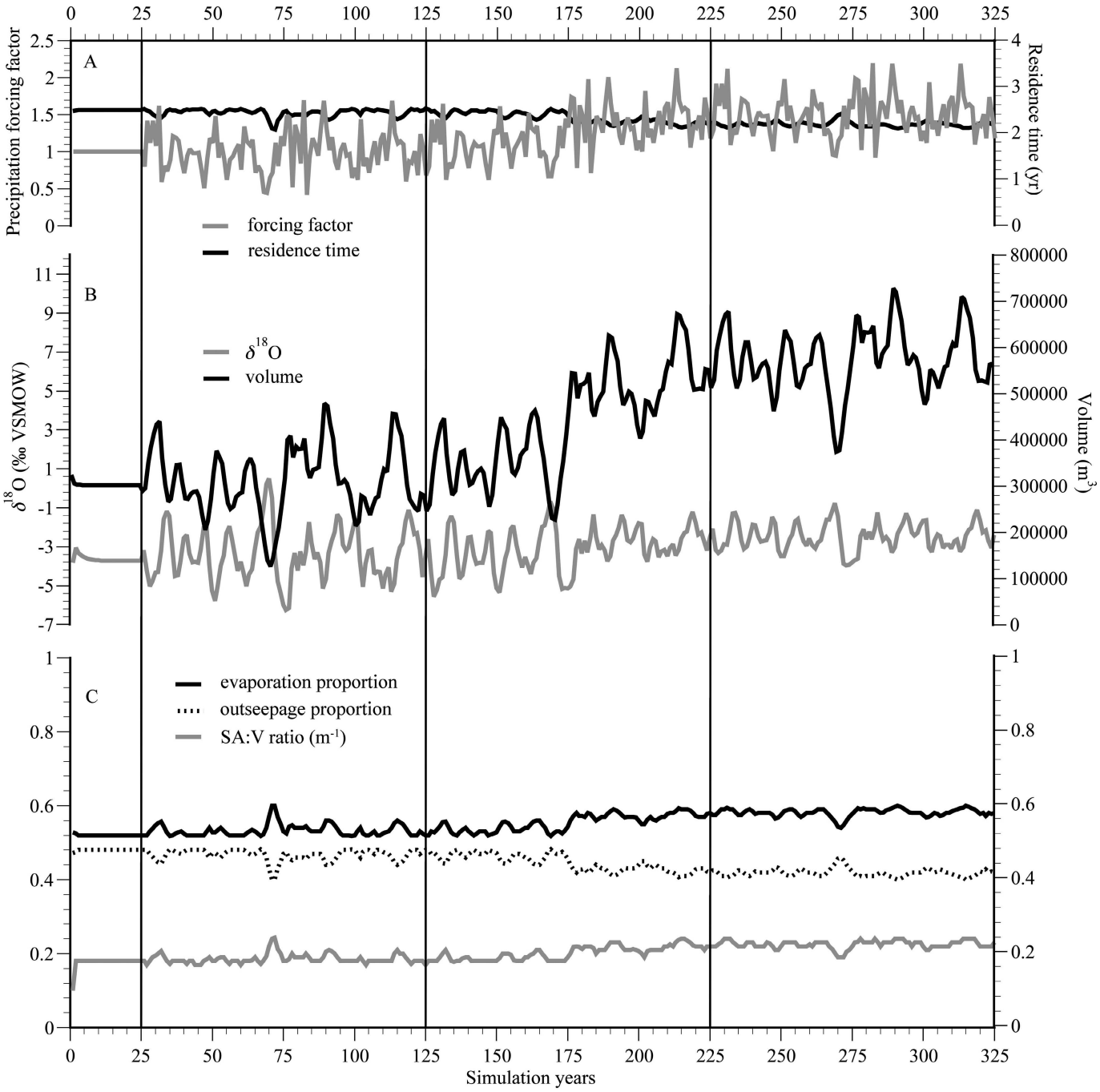

Fig. 5. CL responses to the superimposition of stochastic variations and a mean-state precipitation increase of 50%. Between years 0 and 25, no changes in precipitation were applied. Between years 25 and 125, precipitation was varied stochastically with a mean and standard deviation equal to observed 20th-century values. Between years 125 and 225, mean-state precipitation was incrementally increased by 50% while maintaining stochastic variations applied in years 25–125. Between years 225 and 325, mean-state precipitation was maintained at a value 50% above the 20th-century average while again maintaining stochastic variations applied in the prior 100-yr simulation periods. (A) Superimposed stochastic and mean-state precipitation forcing factors (gray line) and residence times (black line). (B) Average summer (June–August) surface-water δ^{18}O values (gray line) and lake volumes (black line) resulting from described precipitation changes. (C) Lake SA : V ratio values (gray line) and the proportions of water lost to evaporation (black line) and outseepage (dashed line).

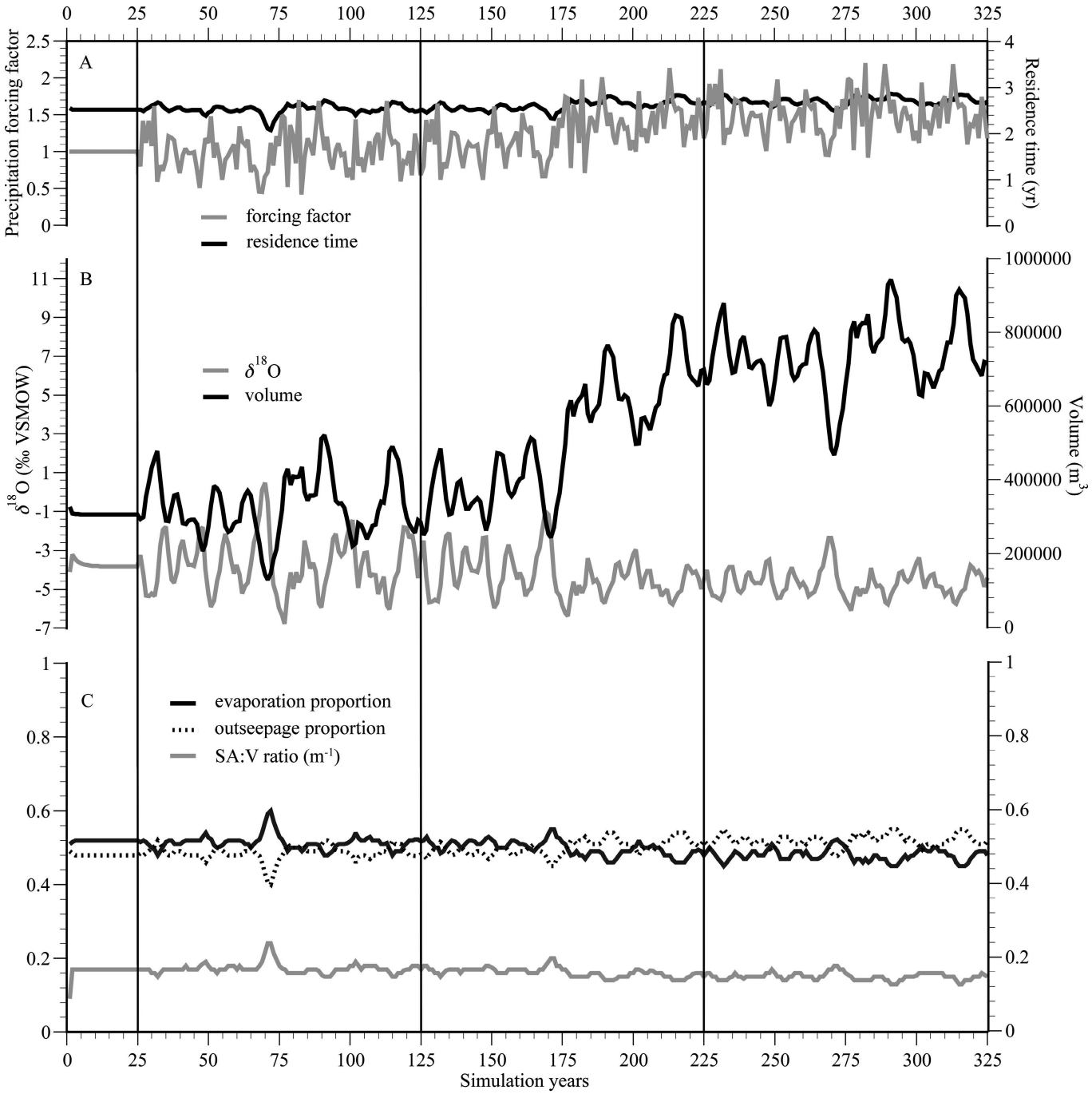

Fig. 6. CL2 responses to the superimposition of stochastic variations and a mean-state precipitation increase of 50%. Between years 0 and 25, no changes in precipitation were applied. Between years 25 and 125, precipitation was varied stochastically with a mean and standard deviation equal to observed 20th-century values. Between years 125 and 225, mean-state precipitation was incrementally increased by 50% while maintaining stochastic variations applied in years 25–125. Between years 225 and 325, mean-state precipitation was maintained at a value 50% above the 20th-century average while again maintaining stochastic variations applied in the prior 100-yr simulation periods. (A) Superimposed stochastic and mean-state precipitation forcing factors (gray line) and residence times (black line). (B) Average summer (June–August) surface-water δ^{18}O values (gray line) and lake volumes (black line) resulting from described precipitation changes. (C) Lake SA : V ratio values (gray line) and the proportions of water lost to evaporation (black line) and outseepage (dashed line).

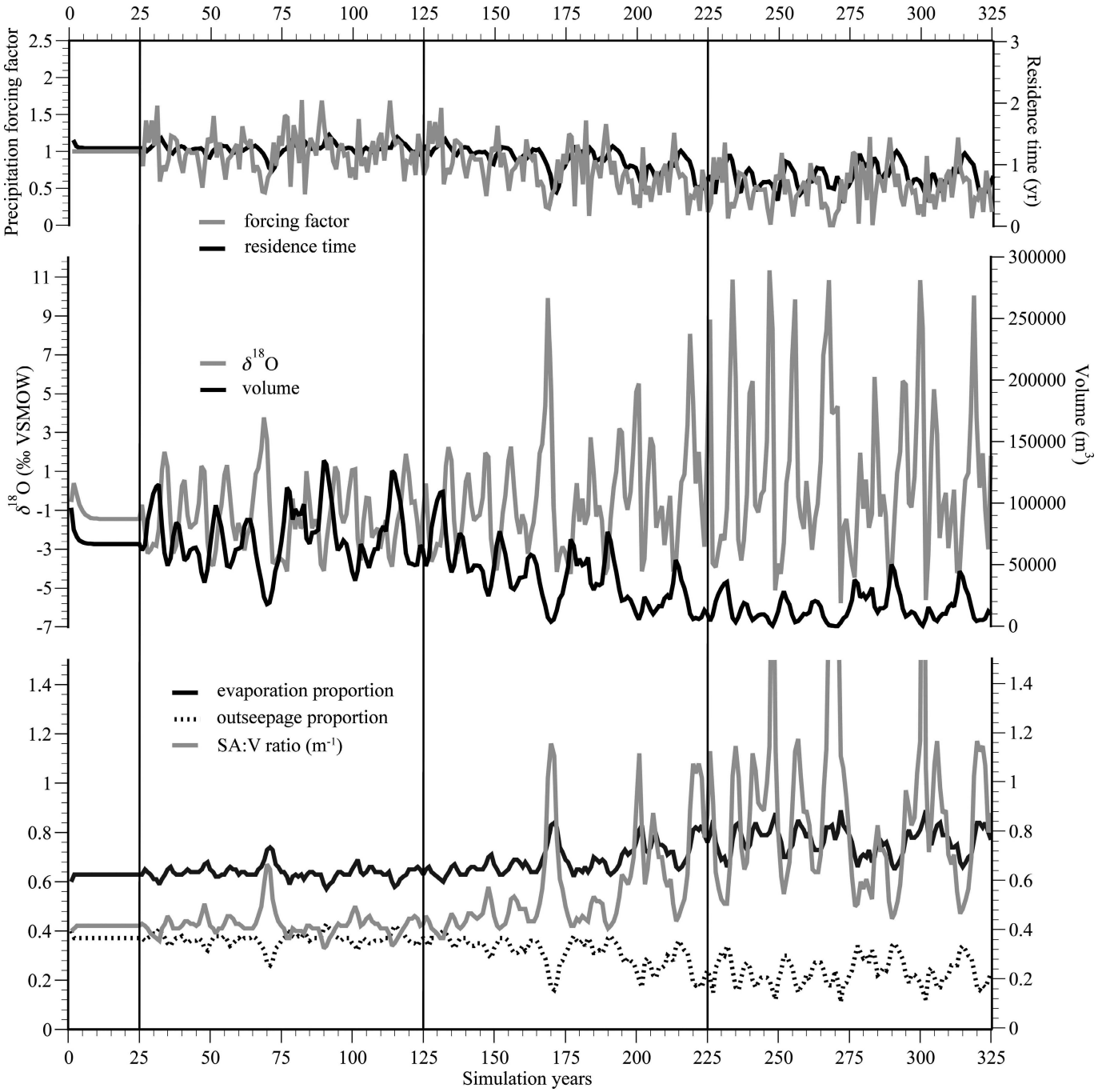

Fig. 7. SL2 responses to the superimposition of stochastic variations and a mean-state precipitation decrease of 50%. Between years 0 and 25, no changes in precipitation were applied. Between years 25 and 125, precipitation was varied stochastically with a mean and standard deviation equal to observed 20th-century values. Between years 125 and 225, mean-state precipitation was incrementally decreased by 50% while maintaining stochastic variations applied in years 25–125. Between years 225 and 325, mean-state precipitation was maintained at a value 50% below the 20th-century average while again maintaining stochastic variations applied in the prior 100-yr simulation periods. (A) Superimposed stochastic and mean-state precipitation forcing factors (gray line) and residence times (black line). (B) Average summer (June–August) surface-water $\delta^{18}O$ values (gray line) and lake volumes (black line) resulting from described precipitation changes. (C) Lake SA : V ratio values (gray line) and the proportions of water lost to evaporation (black line) and outseepage (dashed line).

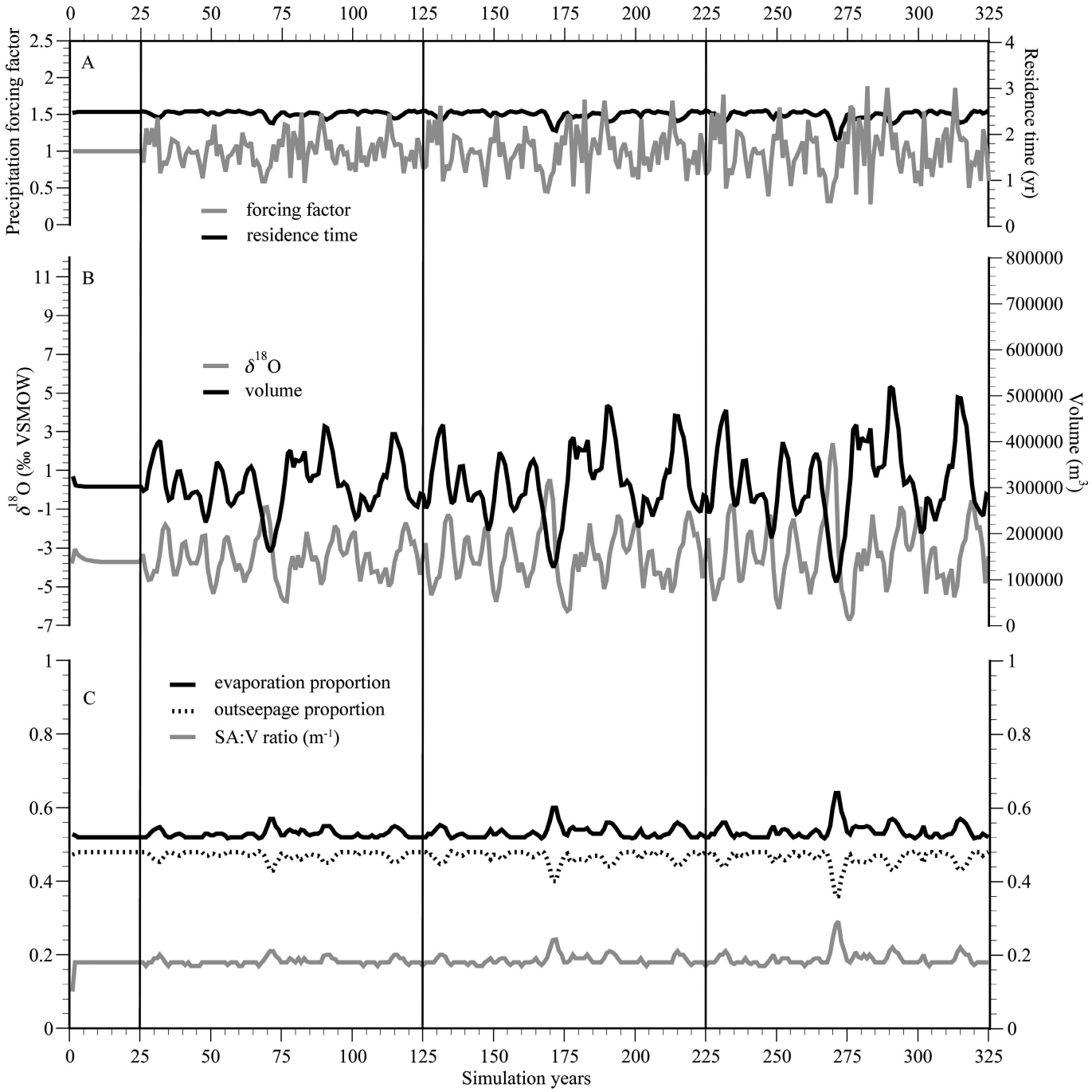

Fig. 8. CL responses to changes in the variance of stochastic precipitation changes. Between years 0 and 25, no changes in precipitation were applied. Between years 25 and 125, precipitation was varied randomly (stochastically) with a standard deviation 25% lower than the observed 20th-century value. Between years 125 and 225, precipitation was varied randomly with a standard deviation equal to the observed 20th-century value. Between years 225 and 325, precipitation was varied randomly with a standard deviation 25% greater than the observed 20th-century value. (A) Stochastic precipitation forcing factors (gray line) and residence times (black line). (B) Average summer (June–August) surface-water δ^{18}O values (gray line) and lake volumes (black line) resulting from the described precipitation changes. (C) Lake SA : V ratio values (gray line) and the proportions of water lost to evaporation (black line) and outseepage (dashed line).

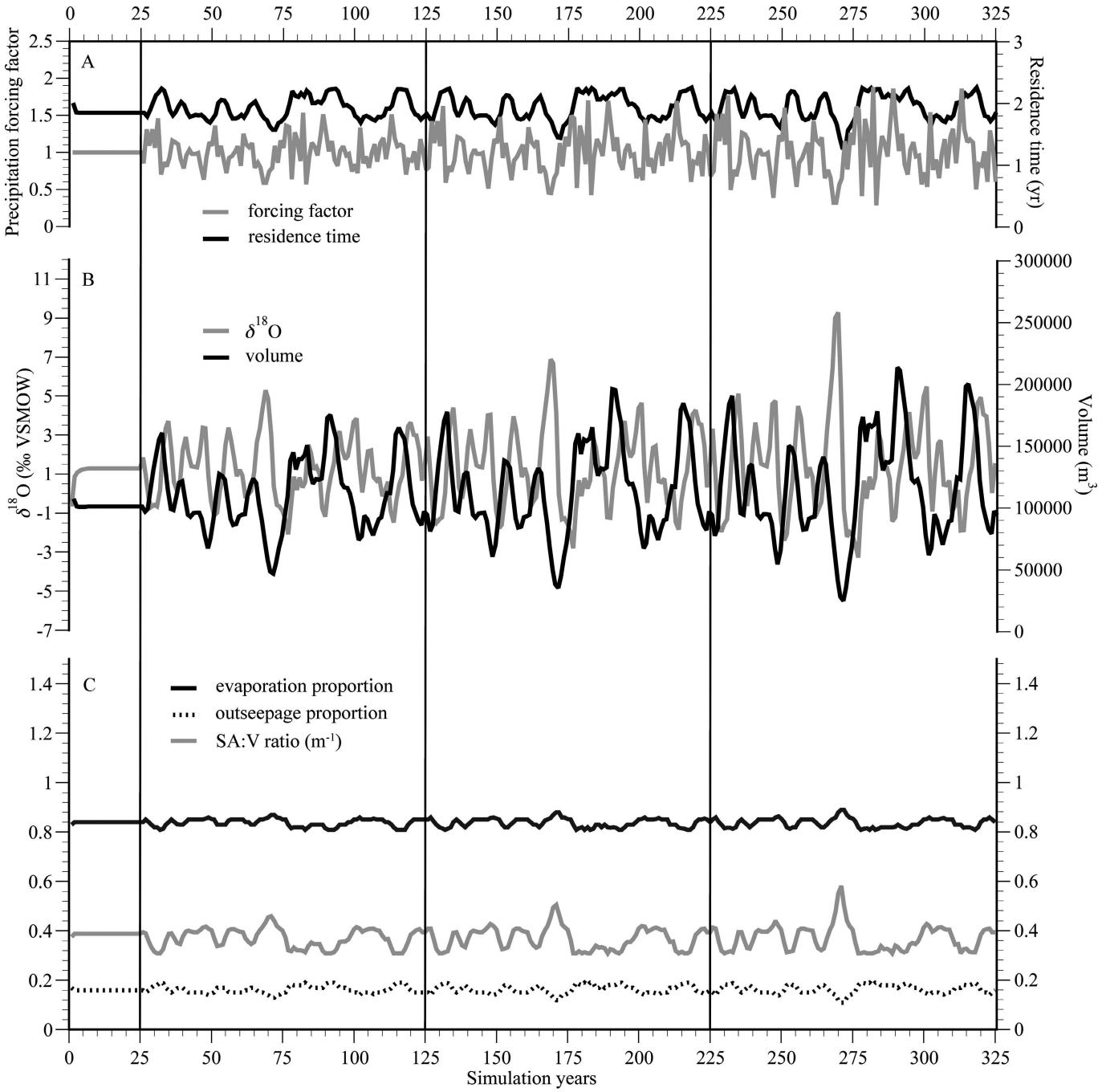

Fig. 9. SL responses to changes in the variance of stochastic precipitation changes. Between years 0 and 25, no changes in precipitation were applied. Between years 25 and 125, precipitation was varied randomly (stochastically) with a standard deviation 25% lower than the observed 20th-century value. Between years 125 and 225, precipitation was varied randomly, with a standard deviation equal to the observed 20th-century value. Between years 225 and 325, precipitation was varied stochastically with a standard deviation 25% greater than the observed 20th-century value. (A) Stochastic precipitation forcing factors (gray line) and residence times (black line). (B) Average summer (June–August) surface-water δ^{18}O values (gray line) and lake volumes (black line) resulting from the described precipitation changes. (C) Lake SA : V ratio values (gray line) and the proportions of water lost to evaporation (black line) and outseepage (dashed line).

at CL, the SA : V ratio increases, which leads to an increase in the proportion of water leaving the lake through evaporation. At SL, however, the response is different in that the low outseepage rate results in an evaporation outflow proportion that is high regardless of the SA : V ratio, resulting in a minimal steady-state $\delta^{18}O$ change.

Lake responses to combined mean-state and stochastic precipitation forcing—A comparison of the SL and CL precipitation variability simulation results reveals several differences between the isotopic and hydrologic responses of the two lakes. Perhaps most notably, in every simulation period of the precipitation change scenarios (both +50% and −50%), the standard deviation of the average summer isotopic $\delta^{18}O$ values at SL was higher than the corresponding value for CL (Table 1). This can be explained by the stronger transient response to hydrologic forcing at SL (*see* Lake responses to mean-state precipitation forcing), which results from the lower volume and residence time and higher SA : V ratio values. A related observation is that, for both SL and CL, as lake volume increases in response to increasing mean-state precipitation, the standard deviation of the summer average $\delta^{18}O$ values decreases, and vice versa. At both CL and SL, as the mean annual precipitation total increases, and the standard deviation of precipitation values remains unchanged, lake level and volume will increase, resulting in volumetric fluxes associated with stochastic variability that are proportionally smaller in comparison to total lake volume. As precipitation amounts decrease, in contrast, the volumetric fluxes associated with stochastic precipitation changes become larger relative to total lake volume.

The summer average $\delta^{18}O$ values of CL and SL also show dissimilarities. Most notably, in every simulation period SL $\delta^{18}O$ values are comparatively higher than CL values. This occurs primarily because SL has a lower outseepage rate and consequently, an evaporative outflow proportion that is higher than that of CL, which leads to greater overall evaporative enrichment of SL lake waters regardless of the precipitation forcing scenario (Table 1).

The similarity in the direction of the SL and CL steady-state responses to mean-state precipitation changes is also conspicuous, in that long-term precipitation increases result in increased lake volumes and summer average $\delta^{18}O$ values, a somewhat counterintuitive result given that decreasing $\delta^{18}O$ values are typically associated with increasing lake volumes. This result can be explained by the interplay between the outseepage flux proportions and the SA : V ratio values which at SL and CL increase with increasing depth above ~ 8.5 m and 12 m, respectively (*see* Lake responses to mean-state precipitation forcing, above).

The CL precipitation reduction scenario provides an example of how the direction of the SA : V ratio can influence lake steady-state $\delta^{18}O$ values. Over the first half of the second simulation period (simulation years 125–175), lake volume decreased while the SA : V ratio varied only slightly, which in turn led to only a small change in the steady-state summer average $\delta^{18}O$ value (Fig. 4). Not until simulation year 175, when lake volume decreased to the extent that the SA : V ratio value began to rapidly increase, did the large increase in the steady-state CL summer average $\delta^{18}O$ value begin.

Additionally, for both CL and SL, a decrease in residence time occurred in response to 50% increases and decreases in mean-state precipitation. In both cases, this can be explained in part by the increase in the SA : V ratio with both increasing and decreasing depth. As lake volume increases, surface area increases to a proportionally greater extent, allowing greater volumetric loss through evaporation and a larger lake-volume–to–outflow ratio.

Hypothetical lake responses to combined mean-state and stochastic precipitation forcing—In the hypothetical CL2 configuration, in which SA : V ratio values increased with increasing depth above 12 m, mean-state precipitation increases resulted in a decrease in steady-state $\delta^{18}O$ values, a response opposite that of the CL configuration under the same precipitation-forcing scenario (Fig. 6). This opposite response can again be explained by the interplay between SA : V ratio values and outseepage flux proportions. In the CL2 configuration, as lake volume increased, SA : V ratio values decreased rather than increased (as in the CL configuration), leading to a decrease in the proportion of water lost through evaporation. Summer average $\delta^{18}O$ values therefore decreased in response to the decrease in evaporative enrichment and the consequent increase in water lost through outseepage.

In the hypothetical SL2 configuration the outseepage rate was increased by a factor of three (i.e., from 0.007 to 0.021) relative to the estimated value for Scanlon Lake. Consequently, the average summer $\delta^{18}O$ values prior to mean-state precipitation forcing were lower due to the relative decrease in the proportion of water lost through evaporation (Fig. 7). Just as the small outseepage rate in the SL simulations resulted in a minimal response to mean-state hydrologic forcing, the relatively large outseepage rate in the SL2 simulations resulted in a substantial isotopic response. This inference is supported by the large increase in summer average $\delta^{18}O$ values and in the evaporation outflow proportion observed during the second and third simulation periods (Table 1).

Lake responses to variance changes in stochastic precipitation forcing—Hydrologic responses to changes in stochastic precipitation were similar at CL and SL in that an increase in the standard deviation of interannual precipitation values led to an increase in average lake volume (Table 1). This apparent steady-state hydrologic sensitivity to stochastic forcing can be explained by mechanisms controlling water delivery to the lake. In accordance with fundamental catchment hydrologic processes, the model calculates runoff on the basis of available water capacity (AWC) and the intra-annual water surpluses and deficits resulting from seasonal variability in precipitation and evapotranspiration. Specifically, when precipitation exceeds evapotranspiration, catchment AWC is reached (i.e., soils are saturated), and runoff to the lake occurs. Conversely, when precipitation does not exceed evapotranspiration, catchment AWC is not reached, and runoff does not occur. One consequence of this simple

hydrologic process is a nonlinear relationship between precipitation and runoff. For example, when soils are saturated, increasing precipitation will result in increasing runoff until precipitation rates decrease (or evapotranspiration rates increase) to a level at which soils are no longer saturated. At this point, further decreases in precipitation are irrelevant in determining the runoff rate, which remains zero until precipitation rates increase (or evapotranspiration rates decrease) to the point at which soils are again saturated. Long-term average lake volume is therefore influenced to a greater extent by the magnitude of positive hydrologic forcing (i.e., precipitation increases) than by the magnitude of negative hydrologic forcing, such that increases in the variance of stochastic forcing result in more frequent high-volume precipitation and runoff events that increase long-term lake volume.

Implications for paleoclimate studies—In the interpretation of closed-basin lake sediment oxygen isotope records a frequent assumption is that long-term (century- to millennial-scale) increases in $\delta^{18}O$ values correspond to decreases in effective moisture or precipitation–evaporation balance. The model simulations of stochastic and mean-state precipitation changes presented here demonstrate that this assumption may not always be valid, as the interplay between outseepage rates and the effect of SA : V ratio changes with depth on evaporative flux proportions can influence steady-state lake-water $\delta^{18}O$ values. Specifically, in lakes with appreciable outseepage rates (such as CL), the extent to which volumetric adjustments will affect evaporation and seepage outflow proportions is in part controlled by the magnitude of the SA : V ratio change. Conversely, in lakes with minimal outseepage (such as SL), the SA : V ratio changes that result from volumetric adjustments will not affect steady-state water $\delta^{18}O$ values because evaporation outflow proportions remain far greater than seepage outflow proportions (no matter the SA : V ratio). Simulation results additionally demonstrate that variability in lake-water $\delta^{18}O$ values is largely controlled by total lake volume and the consequent percentage change in lake volume in response to stochastic variability in hydroclimate. The implications of this inference are twofold, in that given similar catchments, smaller (volumetrically) closed-basin lakes (e.g., SL) will exhibit a larger standard deviation of annual lake-water $\delta^{18}O$ values than will volumetrically larger closed-basin lakes (e.g., CL), and that the standard deviation of annual $\delta^{18}O$ values will increase as lake volume decreases and the consequent percentage changes in lake volume increase in response to stochastic forcing (and vice versa). This latter implication is especially relevant to paleoclimate studies, as changes in the magnitude of closed-basin lake sediment-core oxygen-isotopic variability may reflect past variations in the mean state of hydroclimate and not stochastic variability. When mean-state climate changes are not applied, however, model simulations suggest that lake volumes are controlled largely by stochastic variability, with greater variance in precipitation resulting in greater average lake volume (and vice versa) (Figs. 8, 9; Table 1). Given large enough variance changes and, as a consequence, significantly greater lake volume, this relationship could result in a reduced lake-water oxygen-isotopic response to stochastic forcing (*see* Lake responses to combined mean-state and stochastic precipitation forcing, above).

Given the observations and constraints described above, records of stochastic variability in hydroclimate should ideally be generated from sedimentary deposits within closed-basin lakes with low outseepage rates, high SA : V ratios, and small volumes, all characteristics that lead to large, short-term percentage volumetric changes and correspondingly large isotopic responses. Conversely, mean-state changes in hydroclimate should be reconstructed using sediment records from closed-basin lakes with relatively high outseepage rates, large volumes, and SA : V ratios that vary considerably with changing lake level. In some cases, a lake may be useful for both stochastic and mean-state hydroclimate analyses. CL, for example, has an outseepage rate high enough to cause substantial responses to mean-state, hydroclimatic forcing as well as a small enough volume and high enough SA : V ratio to strongly respond to stochastic forcing.

In many cases, robust paleoclimatic reconstructions may not be developed without isolating the individual components of hydroclimatic change (i.e., mean-state and stochastic variability) by coupling analyses from nearby closed-basin lakes with disparate morphologies, outseepage rates, and consequently varying responses to stochastic and mean-state hydrologic forcing. In the cases such as Scanlon Lake and Castor Lake, which have differing morphologies and outflow dynamics, analysis of sediment core $\delta^{18}O$ records can provide insight into past hydroclimatic conditions and, more importantly, into controlling synoptic-scale climate patterns such as the Pacific Decadal Oscillation (generally, positive PDO phases generally correlate to drought in the Columbia River basin) (Mantua and Hare 2002; Gedalof et al. 2004; Knapp et al. 2004). This is only possible, however, when the hydrologic and isotopic responses of the analyzed lake systems to climate change are well understood.

Acknowledgments

We thank Nathan Stansell, Chris Helander, Jeremy Moberg, Broxton Bird, and Jon Riedel for assistance in the field. We also thank two anonymous reviewers for thoughtful remarks on the manuscript. This work was funded by National Science Foundation Earth System History program grant 0401948 and small grants from the Geological Society of America and the University of Pittsburgh's Henry Leighton Memorial Scholarship and International Studies Fund.

References

Almendinger, J. E. 1993. A groundwater model to explain past lake levels at Parkers Prairie, Minnesota, USA. Holocene **3:** 105–115, doi:10.1177/095968369300300202

Cross, S. L., P. A. Baker, G. O. Seltzer, S. C. Fritz, and R. B. Dunbar. 2001. Late quaternary climate and hydrology of tropical South America inferred from an isotopic and chemical model of Lake Titicaca, Bolivia and Peru. Quaternary Res. **56:** 1–9, doi:10.1006/qres.2001.2244

Donovan, J. J., A. J. Smith, V. A. Panek, D. R. Engstrom, and E. Ito. 2002. Climate-driven hydrologic transients in lake sediment records: calibration of groundwater conditions using 20th century drought. Quat. Sci. Rev. **21:** 605–624, doi:10.1016/S0277-3791(01)00042-7

GAT, J. R. 1970. Environmental isotope balance of Lake Tiberias, p. 109–127. *In* Isotopes in hydrology. IAEA.

GEDALOF, Z., D. L. PETERSON, AND N. J. MANTUA. 2004. Columbia River flow and drought since 1750. J. Am. Water Resour. As. **40:** 1579–1592, doi:10.1111/j.1752-1688.2004.tb01607.x

HENDERSON, A. K., AND B. N. SHUMAN. 2009. Hydrogen and oxygen isotopic compositions of lake water in the western United States. Geol. Soc. Am. Bull. **121:** 1179–1189, doi:10.1130/B26441.1

JOHNSON, D. L., AND D. WATSON-STEGNER. 1987. Evolution model of pedogenesis. Soil Sci. **143:** 349–366, doi:10.1097/00010694-198705000-00005

JONES, M. D., M. J. LENG, N. ROBERTS, M. TURKES, AND R. MOYEED. 2005. A coupled calibration and modeling approach to the understanding of dry-land lake oxygen isotope records. J. Paleolimnol. **34:** 391–411, doi:10.1007/s10933-005-6743-0

KATZ, R. W. 1996. Use of conditional stochastic models to generate climate change scenarios. Climatic Change **32:** 237–255, doi:10.1007/BF00142464

KNAPP, P. A., P. T. SOULÉ, AND H. D. GRISSINO-MAYER. 2004. Occurrence of sustained droughts in the interior Pacific northwest (A.D. 1733–1980) inferred from tree-ring data. J. Climate. **17:** 140–150, doi:10.1175/1520-0442(2004)017<0140:OOSDIT>2.0.CO;2

LENG, M., P. BARKER, P. GREENWOOD, N. ROBERTS, AND J. REED. 2001. Oxygen isotope analysis of diatom silica and authigenic calcite from Lake Pinarbasi, Turkey. J. Paleolimnol. **25:** 343–349, doi:10.1023/A:1011169832093

———, AND J. D. MARSHALL. 2004. Paleoclimate interpretation of stable isotope data from lake sediment archives. Quaternary Sci. Rev. **23:** 811–831, doi:10.1016/j.quascirev.2003.06.012

MANTUA, N. J., AND S. R. HARE. 2002. The Pacific decadal oscillation. J. Oceanogr. **58:** 33–44, doi:10.1023/A:1015820616384

MEARNS, L. O., C. ROSENZWEIG, AND R. GOLDBERG. 1997. Mean and variance change in climate scenarios: Methods, agricultural applications, and measures of uncertainty. Climatic Change **35:** 367–396, doi:10.1023/A:1005358130291

PHAM, S. V., P. R. LEAVITT, S. MCGOWAN, B. WISSEL, AND L. I. WASSENAAR. 2009. Spatial and temporal variability of prairie lake hydrology as revealed using stable isotopes of hydrogen and oxygen. Limnol. Oceanogr. **54:** 101–118.

PHILLIPS, J. D. 1993. Progressive and regressive pedogenesis and complex soil evolution. Quaternary Res. **40:** 169–176, doi:10.1006/qres.1993.1069

RICHARDSON, C. W. 1981. Stochastic simulation of daily precipitation, temperature, and solar radiation. Water Resourc. Res. **17:** 182–190, doi:10.1029/WR017i001p00182

RICKETTS, R. D., AND T. C. JOHNSON. 1996. Climate change in the Turkana basin as deduced from a 4000-yr long $\delta^{18}O$ record. Earth Planet. Sc. Lett. **142:** 7–17, doi:10.1016/0012-821X(96)00094-5

ROSENMEIER, M. F., M. BRENNER, D. A. HODELL, J. B. MARTIN, AND M. W. BINFORD. In press. Quantitative assessments of Holocene environmental change in Petén, Guatemala: Predictive models of catchment hydrology and lake-water $\delta^{18}O$ values. Quaternary Res.

SHAPLEY, M. D., E. ITO, AND J. J. DONOVAN. 2008. Isotopic evolution and climate paleorecords: modeling boundary effects in groundwater-dominated lakes. J. Paleolimnol. **39:** 17–33, doi:10.1007/s10933-007-9092-3

SMITH, A. J., J. J. DONOVAN, E. ITO, AND D. R. ENGSTROM. 1997. Ground-water processes controlling a prairie lake's response to middle Holocene drought. Geology **25:** 391–394, doi:10.1130/0091-7613(1997)025<0391:GWPCAP>2.3.CO;2

———, ———, ———, ———, AND V. A. PANEK. 2002. Climate-driven hydrologic transients in lake sediment records: multiproxy record of mid-Holocene drought. Quat. Sci. Rev. **21:** 625–646, doi:10.1016/S0277-3791(01)00041-5

STEINMAN, B. A., M. F. ROSENMEIER, M. B. ABBOTT, AND D. J. BAIN. 2010. The isotopic and hydrologic response of small, closed-basin lakes to climate forcing from predictive models: application to paleoclimate studies in the upper Columbia River basin. Limnol. Oceanogr. **55:** 2231–2245.

VASSILJEV, J. 1998. The simulated response of lakes to changes in annual and seasonal precipitation: implication for Holocene lake-level changes in northern Europe. Clim. Dynam. **14:** 791–801, doi:10.1007/s003820050255

Associate editor: Roland Psenner

Received: 31 December 2009
Accepted: 31 May 2010
Amended: 15 July 2010